symmetry

MDPI

Article

Enhancing NSGA-II Algorithm through Hybrid Strategy for Optimizing Maize Water and Fertilizer Irrigation Simulation

Jinyang Du [1], Renyun Liu [1,*], Du Cheng [2], Xu Wang [1], Tong Zhang [1] and Fanhua Yu [3]

1 Department of Mathematics, Changchun Normal University, Changchun 130032, China; QX202200197@stu.ccsfu.edu.cn (J.D.); QX202200217@stu.ccsfu.edu.cn (X.W.); QX202200207@stu.ccsfu.edu.cn (T.Z.)
2 School of Artificial Intelligence, Jilin University, Changchun 130012, China; DUGOCD@126.com
3 Jilin Communications Polytechnic, Changchun 130015, China; yufanhua@163.com
* Correspondence: liurenyun@ccsfu.edu.cn

Abstract: In optimization problems, the principle of symmetry provides important guidance. This article introduces an enhanced NSGA-II algorithm, termed NDE-NSGA-II, designed for addressing multi-objective optimization problems. The approach employs Tent mapping for population initialization, thereby augmenting its search capability. During the offspring generation process, a hybrid local search strategy is implemented to augment the population's exploration capabilities. It is crucial to highlight that in elite selection, norm selection and average distance elimination strategies are adopted to strengthen the selection mechanism of the population. This not only enhances diversity but also ensures convergence, thereby improving overall performance. The effectiveness of the proposed NDE-NSGA-II is comprehensively evaluated across various benchmark functions with distinct true Pareto frontier shapes. The results consistently demonstrate that the NDE-NSGA-II method presented in this paper surpasses the performance metrics of the other five methods. Lastly, the algorithm is integrated with the DSSAT model to optimize maize irrigation and fertilization scheduling, confirming the effectiveness of the improved algorithm.

Keywords: NSGA-II; DSSAT model; local search; optimization of irrigation and fertilization

check for updates

Citation: Du, J.; Liu, R.; Cheng, D.; Wang, X.; Zhang, T.; Yu, F. Enhancing NSGA-II Algorithm through Hybrid Strategy for Optimizing Maize Water and Fertilizer Irrigation Simulation. *Symmetry* **2024**, *16*, 1062. https://doi.org/10.3390/sym16081062

Academic Editor: Aviv Gibali

Received: 24 June 2024
Revised: 24 July 2024
Accepted: 1 August 2024
Published: 17 August 2024

Copyright: © 2024 by the authors. Licensee MDPI, Basel, Switzerland. This article is an open access article distributed under the terms and conditions of the Creative Commons Attribution (CC BY) license (https://creativecommons.org/licenses/by/4.0/).

1. Introduction

In the real world, optimization problems frequently manifest as multi-objective optimization problems (MOPs), characterized by a set of conflicting objective functions [1–4]. MOPs are pervasive across numerous application domains, rendering research on intelligent algorithms for addressing MOPs a perennially active area of investigation [5–7]. In MOPs, improving one objective often worsens another, caused by conflicting objectives. In most cases, no single solution can optimize all the objectives at the same time, so the algorithm must find a set of trade-off solutions called the Pareto front (PF) [8,9].

A common challenge in MOPs is devising methods to swiftly attain a convergent solution while also achieving a more evenly distributed solution set [10,11]. To better solve more complex problems, in recent years, various multi-objective evolutionary algorithms (MOEA) have been proposed, including NSGA-II [12], MOEA/D [13], SPEA2 [14], and other algorithms. Since their inception, these algorithms have garnered immense attention from researchers due to their impressive global search performance, high-speed operational efficiency, and straightforward algorithmic framework. These multi-objective optimization algorithms are applied to agricultural models. Zhou and Fan [15] optimized the agricultural industry structure through a genetic-algorithm-based MOP to achieve sustainable development. Llera [16] et al. optimized control settings using the NSGA-II algorithm to help growers achieve maximum yield and minimize costs under greenhouse conditions. Cheng [17] et al. optimized the irrigation and fertilization plan for winter wheat by combining the NSGA-II algorithm with the DSSAT model. Song [18] et al. optimized the spring wheat irrigation plan using the AquaCrop model and NSGA-II algorithm. Liu and Yang [19] constructed a distributed AquaCrop model and NSGA-II for simulation optimization to develop effective irrigation plans. Despite the theoretical and experimental effectiveness of these classic algorithms, they exhibit significant shortcomings in practical applications, particularly regarding convergence speed and solution consistency. Specifically, when addressing high-dimensional and complex problems, the existing algorithms often require extended periods to achieve satisfactory solutions. In practical applications, rapid convergence is essential for conserving computational resources and time. Furthermore, the solutions generated by the current algorithms can vary significantly between different runs, leading to insufficient reliability. Ensuring solution consistency is crucial for maintaining the stability and reproducibility of results.

This article proposes an improved NSGA-II algorithm to address the aforementioned issues. In initializing the population, using the Tent mapping initialization method ensures a more unified initial solution, facilitates exploration of different regions, and enhances the initial searchability. In the adaptive elite selection strategy proposed in this article, in the early stage, the solutions with good convergence and diversity are selected based on norms to enhance convergence and maintain a certain degree of diversity. In the later stage, a selection method based on the average distance elimination strategy is adopted to evenly distribute the population on the Pareto front, which is beneficial for the diversity of the algorithm. Furthermore, within the offspring generation process, a mixed local search strategy is employed. This approach facilitates random updates of the solution between the optimal individual and neighboring individuals, thereby enhancing the solution's search capabilities. Subsequently, the algorithm was combined with the DSSAT [20–22] model to optimize irrigation and fertilization management during the maize growth cycle. The main contributions of this article are summarized as follows: (1) The initialization method of the Tent chaotic mapping was employed for initializing the population. (2) An adaptive elite selection strategy grounded in norm and average distance elimination was formulated to identify superior solutions. (3) A mixed local search strategy was added during the generation of offspring. (4) The algorithm was integrated with the DSSAT model to simulate agricultural scenarios, leading to the development of a successful irrigation and fertilization strategy.

The rest of this article is organized as follows. Section 2 introduces the NSGA-II and its related works. Section 3 provides a comprehensive description of the proposed NDE-NSGA-II, including the applied strategies and a complete framework. Section 4 conducted experiments on the benchmark function, evaluated the performance of NDE-NSGA-II, and discussed the experimental results in detail. Section 6 applies NDE-NSGA-II and the original algorithm to maize yield optimization, proving the feasibility of the algorithm proposed in this paper. Afterwards, the performance of the algorithm is discussed. Finally, this article provides a summary in the sixth section.

2. Related Works

2.1. Multi-Objective Algorithm NSGA-II

NSGA-II is developed based on NSGA, incorporating the principles of nondominated sorting and an elitism strategy. The algorithm calculates the neighborhood density of individuals using the crowding distance (CD). Selection operators for both fitness and diversity are employed to enhance the overall performance of the algorithm.

According to the nondominated sorting strategy of NSGA-II, as illustrated in Figure 1, suppose the population size is N, and Population R_t (with a size of $2N$) is formed by combining the current dominated solution set P_t and the current offspring Q_t. Following the dominance relation, R_t obtains a series of nondominated Pareto solution sets denoted as $F_1, F_2, \ldots$, where F_1 is at the top level. If the quantity of F1 is less than N, all members of F1 are selected into Population P_{t+1}. The remaining members in Population P_{t+1} are chosen from F_2, F_3, and so forth, until the total number of members reaches N. Notably, the order of the first member in F_3 is less than N, while the order of the last member is greater than N. To maintain population diversity, the NSGA-II algorithm employs CD sorting on F_3. Individuals with a larger CD are given priority to enter Population P_{t+1}. The CD calculation method is expressed in Formula (1).

$$n_d = \sum_{m=1}^{M} \frac{f_m(i+1) - f_m(i-1)}{f_m^{max} - f_m^{min}} \tag{1}$$

where f_m^{max} and f_m^{min} are the maximum and minimum of objective function f_m, m is the individual of the solution set, M represents the number of targets.

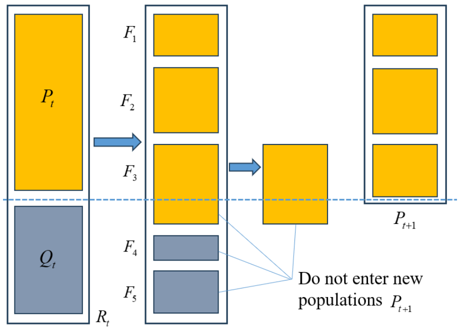

Figure 1. Nondominated sorting strategy of nondominated sorting genetic algorithm II [23] (NSGA-II).

2.2. Problems in CD Sorting of NSGA-II

Following the completion of nondominated sorting, the CD of each solution within the nondominated solution set at the same level is calculated based on the objective space. The CD of the extreme solution (either the maximum or minimum solution across all objectives within the objective space) is consistently set as infinity. For all other solutions, they are sorted based on all objectives, and their CD is defined as the average value of target distances between two adjacent solutions.

In Figure 2, considering eight nondominated solutions, five solutions were selected based on the CD. According to the CD sorting algorithm of NSGA-II, solutions 1, 2, 3, 4, and 8 are chosen. However, it is observed that after the selection, the results of Solutions 4 and 8 are deemed unreasonable due to the sparse distance between them.

Upon the preceding analysis, it is evident that the congestion distance mechanism employed by NSGA-II exhibits uneven distribution issues, potentially compromising the diversity of solutions. Consequently, we present an enhancement strategy for this mechanism in the subsequent section.

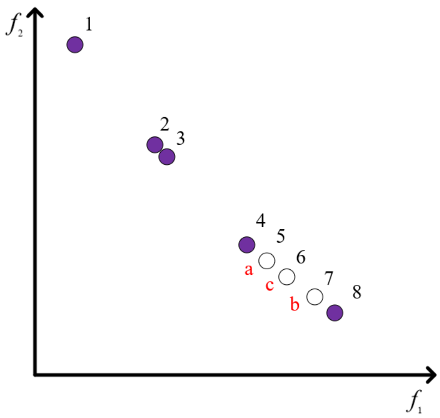

Figure 2. Screening results with NSGA-II. The numbers in the figure denote different individuals, and the letters indicate those that have been removed.

3. The Proposed NDE-NSGA-II

This section provides a comprehensive introduction to the proposed NDE-NSGA-II, with the main objective of enhancing the convergence and diversity of NSGA-II. Firstly, the initialization method of Tent mapping in chaotic mapping was adopted to generate a more uniform population during the initialization stage. Subsequently, a local search strategy and an adaptive elite selection mechanism were adopted to maintain convergence and diversity within the population, ensuring the balance of solutions. Then the overall workflow of NDE-NSGA-II was introduced, including these key enhancements to the traditional NSGA-II model. The overall framework is illustrated in Figure 3.

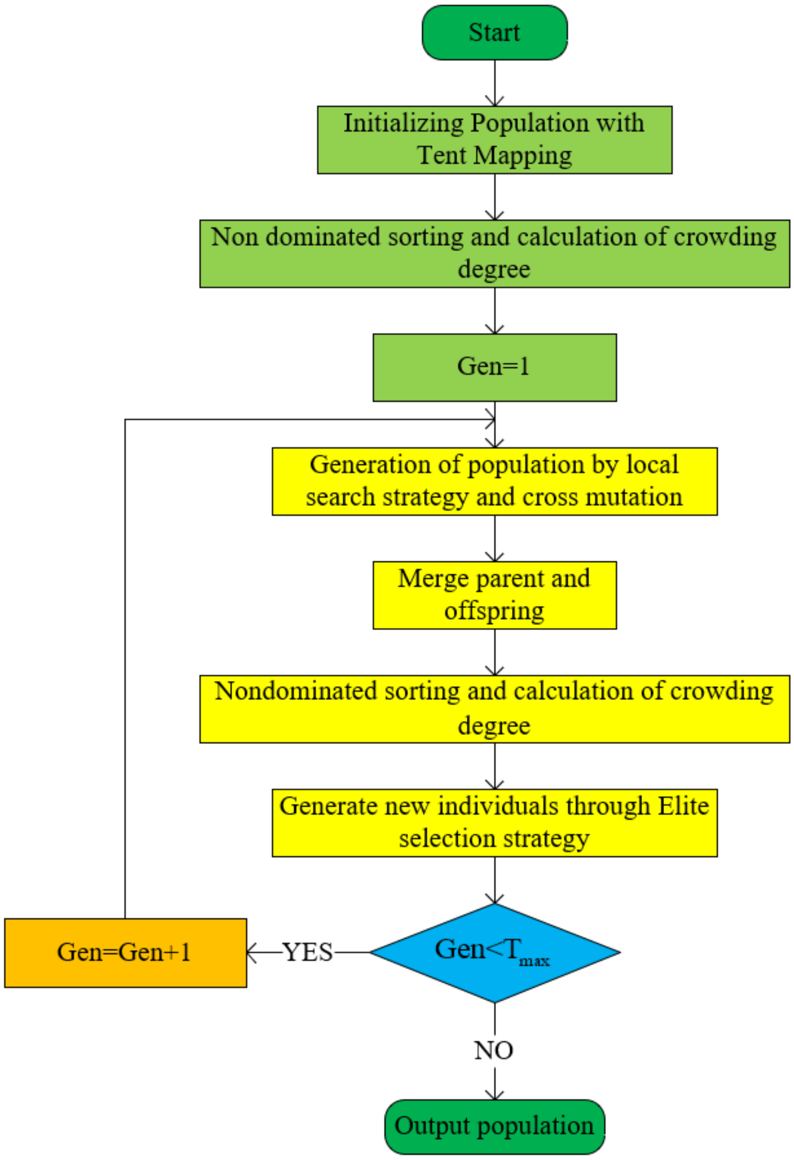

Figure 3. The flow chart of NDE-NSGA-II algorithm.

3.1. Initializing Population with Tent Mapping

Over the past few decades, chaotic mapping [24] has found extensive application across various fields, including parameter optimization, feature selection, and chaos control. The popularity of chaotic mapping arises from three distinctive properties inherent in chaotic mapping sequences: initial value sensitivity, ergodicity, and non-repeatability. Utilizing chaotic mapping in the initialization stage serves to mitigate repetition, fostering a more uniformly distributed initial population. This approach addresses challenges encountered by previous intelligent optimization algorithms during the initialization phase, consequently enhancing the diversity of the decision space. The Tent mapping in chaotic maps has been proven to be an effective initialization method [25].

This article employs the Tent mapping in chaotic mapping for initialization, and the method is outlined as follows:

$$Pop = lb + T(N, dim) \times (ub - lb) \tag{2}$$

In this context, Pop represents the initialized population, u_b and l_b denote the upper and lower bounds of the population, N signifies the number of populations, dim indicates the number of decision variables, and T represents the mapped random number. The formula for calculating T is as follows:

$$T_{n+1} = \begin{cases} \frac{T_n}{\alpha} & T_n < \alpha \\ \frac{1-T_n}{1-\alpha} & T_n \geq \alpha \end{cases} \tag{3}$$

Among them, α = 0.7. The pseudocode for initializing the population is as shown in Algorithm 1.

Algorithm 1 Tent Chaos Initialization

Input: : population size N, decision variables dim, variable upper bound ub, variable lower bound lb
Output: : new population Pop

```
1:  α = 0.7    Tent chaos coefficient
2:  T = rand(N, dim)    Random initialization population
3:  for i = 1 : N do
4:      for j = 2 : dim do
5:          if T_{i,j−1} < α then
6:              T_{i,j} = T_{i,j−1}/α
7:          else
8:              T_{i,j} = (1 − T_{i,j−1})/(1 − α)
9:          end if
10:     end for
11: end for
12: Pop = lb + T × (ub − lb)
```

3.2. Local Search Strategy

In NSGA-II, nondominated sorting is used to assign individuals to different Pareto levels. Utilizing this approach can bolster the algorithm's convergence; however, in instances where the optimization problem exhibits high complexity, it may suffer from inadequate optimization accuracy and susceptibility to local optima. Quadratic interpolation serves as a technique for locating the minimum value point of the objective function, a method previously demonstrated to enhance local exploration capabilities [26]. This paper advances the existing methods by introducing a hybrid local update strategy. In this strategy, particles undergo random updates positioned between the optimal individual and neighboring individuals. The formula for this update strategy is as follows:

$$X_i = \begin{cases} Y_i & \text{rand} < 0.3 \\ Z_i & \text{rand} > 0.3 \end{cases} \tag{4}$$

$$Y_{i,j} = 0.5 \times \frac{(X_{i,j}^2 - X_{m,j}^2) \times f_b + (X_{m,j}^2 - X_{b,j}^2) \times f_i + (X_{b,j}^2 - X_{i,j}^2) \times f_m}{(X_{i,j} - X_{m,j}) \times f_b + (X_{m,j} - X_{b,j}) \times f_i + (X_{b,j} - X_{i,j}) \times f_m} \tag{5}$$

Among these, $X_{i,j}$ represents the current particle, where $X_{m,j}$ and f_m denote the mean individual and fitness values of the j-th dimensional particle, respectively. Furthermore, f_b and $X_{b,j}$ represent random individuals and fitness values among those with Pareto level 1.

$$Z_{i,j} = \begin{cases} X_{i,j} + c_1 \times (X_{n,j} - X_{i,j}) \times (1 - \frac{t}{T})^2 & c_2 > 0.5 \\ X_{i,j} - c_1 \times (X_{n,j} - X_{i,j}) \times (1 - \frac{t}{T})^2 & c_2 < 0.5 \end{cases} \tag{6}$$

c_1 and c_2 are random numbers sampled from the interval [0,1], where t denotes the current iteration number, T represents the maximum iteration number, and $X_{n,j}$ refers to the neighboring individual of the current individual. The above two formulas demonstrate symmetry. The formula is as follows:

$$X_{n,j} = rand(1 - sin(\frac{2t}{T} \times \pi)) \times X_{i,j} \tag{7}$$

In the aforementioned update strategies, individuals constituting 0.4 N are selected for local updates. The pseudocode for a local search is as shown in Algorithm 2.

Algorithm 2 The local searching strategy

Input: : individuals at boundary and center points POp, offspring size N
Output: : population determined by local algorithm Nnf
for $i = 1 : N$ **do**
    Randomly select an individual X from Pop
    $index$=$rand(dim)$
    x=X_{index}
    Conduct local updates based on Formula (4).
    X_{index}=x_new
end for
Nnf=Pop

3.3. Convergence and Diversity Measures

The NSGA-II algorithm utilizes the Pareto dominance method for solution selection, effectively maintaining convergence. However, the selection of solutions from the last layer can impact the algorithm's convergence and diversity during elite selection. To address this, the article introduces enhancements to the elite selection strategy. The convergence degree of each solution in population P is assessed using the p-norm value of the objective vector:

$$Norm(x) = \parallel F(x)^n \parallel_p = \sum_{i=1}^{M} (f_i^n(x)^p)^{(1/p)} \tag{8}$$

where $F_n(x)$ is the objective vector of solution x after the normalization and M is the number of objectives. The most commonly used norm values are $p = 1$ and $p = 2$. In this context, we opt for p = 2. A smaller $Norm$ value of solution x indicates its better convergence performance.

In the initial stages of population iteration, to guarantee that the algorithm can sustain both convergence and substantial diversity, the formula for selecting based on the norm and crowding distance is as follows:

$$f(x) = -Norm(x) \times \alpha + CD(x) \times \beta \tag{9}$$

Among them, $a = 0.8, b = 0.2$.

The smaller $Norm(x)$, the better, and the larger $CD(x)$, the better. Therefore, a larger $f(x)$ is better. Based on this, when selecting a solution, we choose a larger $f(x)$.

The NSGA-II algorithm ensures diversity through a crowding distance strategy. However, as previously discussed, when the distance between two individuals is very close, and the crowding distance is large, this method may struggle to effectively preserve population diversity. This article introduces a strategy based on the balance of the distance between individuals. Initially, the individual with the smaller crowding distance among two individuals with the closest distance is eliminated. This process is repeated sequentially until the desired number of populations is reached. Illustrated in Figure 4, the initial elimination includes individual 3, followed by the sequential elimination of individuals 5 and 7. The final selection comprises individuals 1, 2, 4, 6, and 8, resulting in a more uniform distance between populations and better preservation of diversity.

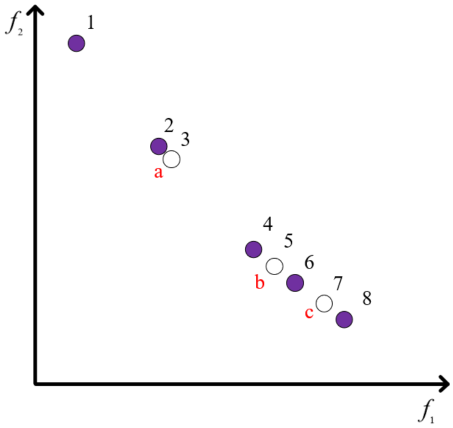

Figure 4. Screening results with average distance elimination method. The numbers in the figure denote different individuals, and the letters indicate those that have been removed.

This article employs the following formula to determine whether to conduct convergence analysis or diversity analysis:

$$P = M \times (r_a - \frac{(r_a - r_b) \times t}{T} \times \frac{n}{N}) \tag{10}$$

Among these variables, M represents the number of targets, with the values of r_a and b_a set to 0.8 and 0.3, respectively. n denotes the count of individuals with Pareto level 1 within the population, while N represents the total number of populations. The pseudocode for convergence and diversity is presented in Algorithm 3.

Algorithm 3 Elitist selection

Input: population size N, combined population $combine\_X$, adaptive probability P
Output: updated population X

$X = 0$
$current\_N = 0$
for i=1 : max_rank **do**
    $current\_N = size(combine\_X_i)$
    if $current\_N \leq N$ **then**
        $X = X + combine\_X_i$
    else
        $remain\_N = N - current\_N$
        if $rand < P$ **then**
            Update individuals according to Equation (9)
        else
            while $size(combine\_X_i)! = remain\_N$ **do**
                $Sort(combine\_X_i)$ Sort based on the distance of each individual
                $delete(min(combine\_X_i)))$
            end while
            $X = X + combine\_X_i$
        end if
    end if
end for

4. Algorithm Comparison

In this section, a set of diverse benchmark tests was conducted to evaluate the performance of NDE-NSGA-II across ZDT [27] to DTLZ [28] functions. The experimental results involved a comparison with four well-established algorithms, NSGA-II, CDE-NSGA-II [23], MOEA/D, and SPEA2, alongside a novel algorithm, CMWOA [29], which incorporates a competition mechanism.

4.1. Indicators for Evaluation

Firstly, this section introduces commonly used indicators for evaluating algorithm performance. In the realm of multi-objective problems (MOPs), the Pareto front (PF) is a crucial concept. Essentially, PF reflects the quality of the Pareto set obtained by the algorithm. The properties of Pareto sets can be described in terms of convergence, diffusion, and uniformity [30], where diffusion and uniformity are denoted as diversity.

To evaluate convergence, this article adopts the indicator GD+ [31], which can be seen as an improvement on the calculation method of the change in distance of the indicator GD. It can better evaluate the convergence degree of the solution than GD. The smaller the value of GD+, the better the solution set.

In terms of diversity, the CPF [32] value is chosen as the performance indicator, with the main idea of projecting the m-dimensional solution onto the M-1 dimensional space. The Pareto set with better diversity results in a higher CPF value.

HV [33] is a comprehensive evaluation indicator for multi-objective optimization algorithms that are sensitive to advantageous relationships. Once a solution set advances in dominance, HV returns a higher value. Meanwhile, due to the important position of dominance in the Pareto set, HV also reflects other performances to a certain extent.

Beyond the aforementioned metrics, we also deliberated on the quantity of offspring discarded or generated by each algorithm within the mutation strategy.

4.2. Convergence Evaluation of Different Algorithms on ZDT and DTLZ Test Problems

Table 1 displays the average GD+ values, accompanied by standard deviations (in parentheses), for the four algorithms, with optimal values highlighted in bold font. Furthermore, a Wilcoxon rank-sum test was performed at a significance level of 0.05. Symbols such as "+", "−", and "=" in the final row denote whether the respective algorithm is significantly superior, significantly inferior, or similar to the proposed NDE-NSGA-II.

Table 1 illustrates that for GD+, NDE-NSGA-II achieved superior results in 5 instances, while NSGA-II, MOEA/D, SPEA, CDE-NSAG-II, and CMWOA secured 1, 3, 0, 0 and 3 best results, respectively. Notably, referencing the information in Table 1, it can be inferred that the proposed NDE-NSGA-II is well-suited for addressing problems with a non-uniform search space and local Pareto front, as observed in ZDT4, ZDT6, DTLZ1, and DTLZ2. However, when confronted with Pareto front problems featuring discrete features like ZDT3 and DTLZ7, NDE-NSGA-II exhibits a comparatively poorer performance. Moreover, results from Wilcoxon's rank-sum test demonstrate that NDE-NSGA-II significantly outperforms the other three methods in more than half of the 12 benchmark functions. This indicates that the NDE-NSGA-II algorithm proposed in this paper emerges as a competitive and effective solution.

Table 1. GD+ values of the proposed NDE-NSGA-II and three multi-objective algorithms.

	D	NSGA-II	MOEA/D	SPEA2	CDE-NSGA-II	CMWOA	NDE-NSGA-II
ZDT1	30	1.1801×10^{-2} $(2.56 \times 10^{-3})-$	7.5242×10^{-2} $(3.78 \times 10^{-2})-$	1.4196×10^{-2} $(2.63 \times 10^{-3})-$	8.8438×10^{-3} $(8.28 \times 10^{-4})-$	3.6228×10^{-4} $(1.09 \times 10^{-4})+$	6.5618×10^{-4} (1.92×10^{-4})
ZDT2	30	1.3028×10^{-2} $(3.38 \times 10^{-3})-$	2.1120×10^{-3} $(2.21 \times 10^{-3})-$	1.1928×10^{-2} $(4.24 \times 10^{-3})-$	1.2578×10^{-2} $(1.77 \times 10^{-3})-$	2.5870×10^{-4} $(1.12 \times 10^{-4})-$	2.2736×10^{-4} (8.81×10^{-5})
ZDT3	30	6.2900×10^{-3} $(4.67 \times 10^{-3})-$	7.5059×10^{-2} $(2.67 \times 10^{-2})-$	1.6723×10^{-3} $(9.49 \times 10^{-3})+$	6.5377×10^{-3} $(5.17 \times 10^{-4})-$	2.1435×10^{-4} $(6.90 \times 10^{-5})+$	3.0208×10^{-3} (2.86×10^{-4})
ZDT4	10	2.7336×10^{-3} $(1.39 \times 10^{-3})-$	1.9089×10^{-2} $(1.82 \times 10^{-2})-$	1.8403×10^{-1} $(1.19 \times 10^{-1})-$	7.2919×10^{-5} $(3.80 \times 10^{-5})=$	2.6171×10^{-1} $(2.05 \times 10^{-1})-$	6.6700×10^{-5} (4.22×10^{-5})
ZDT6	10	5.9099×10^{-2} $(2.59e \times 10^{-2})-$	7.6242×10^{-2} $(2.50 \times 10^{-2})-$	5.8502×10^{-2} $(2.86 \times 10^{-2})-$	1.4148×10^{-1} $(4.90 \times 10^{-2})-$	1.5845×10^{-1} $(1.67 \times 10^{-2})-$	2.4991×10^{-4} (1.47×10^{-4})
DTLZ1	7	1.5090×10^{-2} $(6.28 \times 10^{-2})-$	3.2258×10^{-3} $(1.73 \times 10^{-3})-$	1.1246×10^{-1} $(1.84 \times 10^{-1})-$	$.6833 \times 10^{-2}$ $(8.51 \times 10^{-2})-$	5.6172×10^{-1} $(5.34 \times 10^{-1})-$	2.4667×10^{-3} (1.16×10^{-3})
DTLZ2	12	1.0877×10^{-2} $(9.51 \times 10^{-4})=$	4.6049×10^{-3} $(6.05 \times 10^{-4})+$	5.4658×10^{-2} $(4.57 \times 10^{-4})-$	1.3317×10^{-2} $(1.73 \times 10^{-3})=$	3.1309×10^{-2} $(3.27 \times 10^{-3})-$	1.0645×10^{-2} (1.70×10^{-3})
DTLZ3	12	2.4541×10^{-1} $(5.12e \times 10^{-1})+$	9.8374×10^{-1} $(1.13 \times 10^{0})-$	7.5176×10^{0} $(3.57 \times 10^{0})-$	$1.9417e \times 10^{0}$ $(2.93 \times 10^{0})-$	2.4602×10^{1} $(3.41 \times 10^{1})-$	6.0531×10^{-1} $(8.26 \times 10^{-1}$
DTLZ4	12	9.2717×10^{-3} $(2.88 \times 10^{-3})=$	1.7034×10^{-3} $(2.13 \times 10^{-3})+$	2.0093×10^{-1} $(2.26 \times 10^{-1})-$	1.2253×10^{-2} $(3.76 \times 10^{-3})-$	4.0307×10^{-2} $(8.06 \times 10^{-3})-$	8.9998×10^{-3} (3.09×10^{-3})
DTLZ5	12	1.6588×10^{-3} $(3.60 \times 10^{-4})=$	2.3254×10^{-4} $(1.88 \times 10^{-4})+$	5.2708×10^{-3} $(3.00 \times 10^{-4})-$	1.6606×10^{-3} $(2.55 \times 10^{-4})=$	1.2031×10^{-2} $(2.07 \times 10^{-3})-$	1.5690×10^{-3} (3.00×10^{-4})
DTLZ6	12	2.9192×10^{-5} $(4.50 \times 10^{-5})-$	1.8013×10^{-1} $(4.84 \times 10^{-1})-$	2.8984×10^{-2} $(1.35 \times 10^{-1})-$	8.3978×10^{-5} $(3.71 \times 10^{-4})-$	2.1359×10^{-5} $(1.41 \times 10^{-6})-$	8.6511×10^{-6} (5.41×10^{-7})
DTLZ7	12	5.1449×10^{-2} $(1.10 \times 10^{-2})+$	1.6310×10^{-2} $(4.30 \times 10^{-3})+$	8.1079×10^{-2} $(1.43 \times 10^{-1})+$	1.5389×10^{-2} $(2.84 \times 10^{-2})-$	1.1640×10^{-2} $(2.09 \times 10^{-3})+$	9.6279×10^{-2} (2.51×10^{-2})
+/−/=		2/7/3	4/8/0	2/10/0	0/9/3	3/9/0	

4.3. Diversity Evaluation of Different Algorithms on ZDT and DTLZ Test Problems

Concerning diversity, as indicated by the CPF values in Table 2, the proposed NDE-NSGA-II algorithm outperforms the other five algorithms. It secures the first rank among seven benchmark tests and the second rank among two test functions.

Table 2. CPF values of the proposed NDE-NSGA-II and three multi-objective algorithms.

	D	NSGA-II	MOEA/D	SPEA2	CDE-NSGA-II	CMWOA	NDE-NSGA-II
ZDT1	30	6.8546×10^{-1} $(2.76 \times 10^{-2})-$	1.7925×10^{-1} $(8.16 \times 10^{-2})-$	8.0205×10^{-1} $(2.58 \times 10^{-2})-$	8.3221×10^{-1} $(1.95 \times 10^{-2})-$	8.7450×10^{-1} $(9.60 \times 10^{-3})=$	8.7580×10^{-1} (8.94×10^{-3})
ZDT2	30	6.4410×10^{-1} $(7.42 \times 10^{-2})-$	6.2313×10^{-3} $(8.72 \times 10^{-3})-$	7.2467×10^{-1} $(4.44 \times 10^{-2})-$	7.7441×10^{-1} $(2.79 \times 10^{-2})-$	8.7093×10^{-1} $(8.81 \times 10^{-3})=$	8.6470×10^{-1} (1.09×10^{-2})
ZDT3	30	6.6189×10^{-1} $(3.87 \times 10^{-2})+$	1.1442×10^{-1} $(5.97e \times 10^{-2})-$	7.0745×10^{-1} $(5.33 \times 10^{-2})+$	5.9863×10^{-1} $(3.30 \times 10^{-2})=$	8.9315×10^{-1} $(9.73 \times 10^{-3})+$	6.1488×10^{-1} (5.12×10^{-2})
ZDT4	10	6.7576×10^{-1} $(2.98 \times 10^{-2})-$	4.7501×10^{-1} $(1.59 \times 10^{-1})-$	3.1359×10^{-1} $(9.78 \times 10^{-2})-$	7.6621×10^{-1} $(1.94 \times 10^{-2})-$	4.6558×10^{-1} $(2.16 \times 10^{-1})-$	8.7401×10^{-1} (8.41×10^{-3})
ZDT6	10	5.1181×10^{-1} $(5.75 \times 10^{-2})-$	2.7228×10^{-1} $(1.13 \times 10^{-1})-$	5.0701×10^{-1} $(4.77 \times 10^{-2})-$	5.5266×10^{-1} $(6.90 \times 10^{-2})-$	8.4110×10^{-1} $(2.95 \times 10^{-2})-$	8.7239×10^{-1} (9.44×10^{-3})
DTLZ1	7	2.9803×10^{-1} $(4.97 \times 10^{-2})-$	7.0126×10^{-1} $(4.40 \times 10^{-3})+$	3.5206×10^{-1} $(2.17 \times 10^{-1})-$	3.0072×10^{-1} $(6.34 \times 10^{-2})-$	2.9647×10^{-1} $(2.33 \times 10^{-1})-$	5.9606×10^{-1} (2.68×10^{-2})
DTLZ2	12	3.2695×10^{-1} $(3.54 \times 10^{-2})-$	7.0787×10^{-1} $(6.26 \times 10^{-3})+$	7.1574×10^{-1} $(2.83 \times 10^{-2})+$	$3.4783e \times 10^{-1}$ $(3.56 \times 10^{-2})-$	6.6517×10^{-1} $(2.38 \times 10^{-2})+$	6.1444×10^{-1} (3.06×10^{-2})
DTLZ3	12	2.8899×10^{-1} $(7.70 \times 10^{-2})-$	4.3226×10^{-1} $(1.71 \times 10^{-1})-$	1.0824×10^{-1} $(5.32 \times 10^{-2})-$	3.1697×10^{-1} $(1.28 \times 10^{-1})-$	4.6823×10^{-1} $(1.63 \times 10^{-1})-$	4.8327×10^{-1} (1.75×10^{-1})
DTLZ4	12	3.1499×10^{-1} $(1.11 \times 10^{-1})-$	2.0613×10^{-1} $(3.01 \times 10^{-1})-$	4.9790×10^{-1} $(3.20 \times 10^{-1})-$	3.3847×10^{-1} $(8.73 \times 10^{-2})-$	6.2879×10^{-1} $(2.83 \times 10^{-2})=$	6.3433×10^{-1} (2.97×10^{-2})
DTLZ5	12	7.8294×10^{-1} $(3.54 \times 10^{-2})-$	8.1416×10^{-2} $(3.69 \times 10^{-2})-$	9.4421×10^{-1} $(1.32 \times 10^{-2})-$	9.1363×10^{-1} $(1.24 \times 10^{-2})-$	9.0961×10^{-1} $(2.74 \times 10^{-2})-$	9.5135×10^{-1} (7.11×10^{-3})
DTLZ6	12	6.7924×10^{-1} $(6.48 \times 10^{-2})-$	1.5450×10^{-1} $(1.80 \times 10^{-1})-$	9.2164×10^{-1} $(4.13 \times 10^{-2})-$	8.9498×10^{-1} $(1.54 \times 10^{-2})-$	9.1266×10^{-1} $(8.00 \times 10^{-3})-$	9.5063×10^{-1} (6.60×10^{-3})
DTLZ7	12	4.4126×10^{-1} $(4.01 \times 10^{-2})+$	2.6965×10^{-1} $(3.39 \times 10^{-2})=$	6.2981×10^{-1} $(1.13 \times 10^{-1})+$	1.8519×10^{-1} $(5.49e \times 10^{-2})-$	8.0188×10^{-1} $(8.17 \times 10^{-2})+$	2.4661×10^{-1} (6.78×10^{-2})
+/−/=		2/10/0	2/9/1	3/9/0	0/11/1	3/6/3	

An examination of the results from the rank-sum test indicates that the NDE-NSGA-II proposed in this article significantly surpasses NSGA-II, MOEA/D, SPEA2, CDE-NSGA-II, and CMWOA on 10, 9, 9, 11, and 6 benchmarks, respectively. Notably, in most test functions, the NDE-NSGA-II algorithm demonstrates both high convergence and high diversity. This further substantiates that NDE-NSGA-II can achieve commendable convergence while concurrently maintaining high diversity. Moreover, it is crucial to highlight that the CPF index effectively neutralizes the impact of convergence, providing a reliable assessment of diversity. This suggests that the adopted strategy has indeed played a pivotal role in enhancing population diversity and convergence.

4.4. Comprehensive Evaluation of Different Algorithms on ZDT and DTLZ Test Problems

As previously discussed, the HV value functions as a comprehensive indicator that reflects the overall performance of multi-objective algorithms. The algorithm's overall performance improves with an increase in the value of HV.

Table 3 presents the experimental results of HV values. It is evident from the table that the proposed NDE-NSGA-II surpasses NSGA-II in ten instances, MOEA/D in nine instances, SPEA2 in ten instances, CDE-NSGA-II in eleven instances, and CMWOA's HV value in nine instances. It is noteworthy that among the twelve examples, the proposed NDE-NSGA-II secures the top rank in six test functions.

Table 3. HV values of the proposed NDE-NSGA-II and three multi-objective algorithms.

	D	NSGA-II	MOEA/D	SPEA2	CDE-NSGA-II	CMWOA	NDE-NSGA-II
ZDT1	30	7.0524×10^{-1}	5.4399×10^{-1}	7.0400×10^{-1}	7.0929×10^{-1}	7.2012×10^{-1}	7.1989×10^{-1}
		$(3.16 \times 10^{-3})-$	$(6.02 \times 10^{-2})-$	$(3.56 \times 10^{-3})-$	$(1.27 \times 10^{-3})-$	$(1.43 \times 10^{-4})=$	(1.99×10^{-4})
ZDT2	30	4.1906×10^{-1}	1.0257×10^{-1}	4.2034×10^{-1}	4.2709×10^{-1}	4.4480×10^{-1}	4.4488×10^{-1}
		$(2.54 \times 10^{-2})-$	$(1.35 \times 10^{-2})-$	$(6.61 \times 10^{-3})-$	$(6.21 \times 10^{-3})-$	$(1.47 \times 10^{-4})=$	(9.95×10^{-5})
ZDT3	30	5.7787×10^{-1}	5.6843×10^{-1}	5.9423×10^{-1}	5.7400×10^{-1}	5.8321×10^{-1}	5.7821×10^{-1}
		$(1.93 \times 10^{-2})=$	$(6.44 \times 10^{-2})-$	$(2.45 \times 10^{-2})+$	$(8.99 \times 10^{-4})=$	$(1.28 \times 10^{-4})+$	(6.09×10^{-3})
ZDT4	10	7.1643×10^{-1}	6.8649×10^{-1}	5.1044×10^{-1}	7.1913×10^{-1}	4.4701×10^{-1}	7.2048×10^{-1}
		$(1.76 \times 10^{-3})-$	$(2.59 \times 10^{-2})-$	$(1.29 \times 10^{-1})-$	$(3.84 \times 10^{-5})=$	$(1.66 \times 10^{-1})-$	(5.05×10^{-5})
ZDT6	10	3.1969×10^{-1}	2.7870×10^{-1}	3.1472×10^{-1}	2.5339×10^{-1}	3.8867×10^{-1}	3.8870×10^{-1}
		$(2.98 \times 10^{-2})-$	$(2.95 \times 10^{-2})-$	$(3.49 \times 10^{-2})-$	$(4.50 \times 10^{-2})-$	$(1.87 \times 10^{-4})=$	(1.79×10^{-4})
DTLZ1	7	8.0353×10^{-1}	8.3780×10^{-1}	6.5584×10^{-1}	7.9397×10^{-1}	3.1433×10^{-1}	8.3594×10^{-1}
		$(9.10 \times 10^{-1})-$	$(2.96 \times 10^{-3})=$	$(2.51 \times 10^{-1})-$	$(1.20 \times 10^{-1})-$	$(3.76 \times 10^{-1})-$	(2.39×10^{-3})
DTLZ2	12	5.2846×10^{-1}	5.5490×10^{-1}	5.4292×10^{-1}	5.2397×10^{-1}	5.2613×10^{-1}	5.4495×10^{-1}
		$(4.17 \times 10^{-3})-$	$(8.96 \times 10^{-4})+$	$(1.44 \times 10^{-3})=$	$(4.39 \times 10^{-3})-$	$(4.52 \times 10^{-3})-$	(2.35×10^{-3})
DTLZ3	12	4.1495×10^{-1}	2.0737×10^{-1}	0.0000×10^{0}	2.4195×10^{-1}	6.9750×10^{-2}	3.3573×10^{-1}
		$(1.64 \times 10^{-1})+$	$(2.31 \times 10^{-1})-$	$(0.00 \times 10^{0})-$	$(2.17 \times 10^{-1})-$	$(1.81 \times 10^{-1})-$	(2.12×10^{-1})
DTLZ4	12	5.1554×10^{-1}	3.6056×10^{-1}	4.9017×10^{-1}	5.1736×10^{-1}	5.2232×10^{-1}	5.3118×10^{-1}
		$(5.78 \times 10^{-2})-$	$(1.66 \times 10^{-1})-$	$(9.55 \times 10^{-2})-$	$(3.49 \times 10^{-2})-$	$(5.86 \times 10^{-3})-$	(4.99×10^{-2})
DTLZ5	12	1.9844×10^{-1}	1.8256×10^{-1}	1.9840×10^{-1}	1.9899×10^{-1}	1.9399×10^{-1}	1.9899×10^{-1}
		$(2.71 \times 10^{-4})=$	$(4.25 \times 10^{-4})-$	$(3.76 \times 10^{-4})=$	$(2.06 \times 10^{-4})=$	$(1.43 \times 10^{-3})-$	(1.81×10^{-4})
DTLZ6	12	1.9946×10^{-1}	1.5260×10^{-1}	1.9309×10^{-1}	1.9921×10^{-1}	2.0018×10^{-1}	2.0024×10^{-1}
		$(1.32 \times 10^{-4})-$	$(6.17 \times 10^{-2})-$	$(3.65 \times 10^{-2})-$	$(5.51 \times 10^{-3})-$	$(3.47 \times 10^{-5})=$	(2.26×10^{-5})
DTLZ7	12	2.4741×10^{-1}	2.3085×10^{-1}	2.5446×10^{-1}	1.5659×10^{-1}	2.7467×10^{-1}	1.6271×10^{-1}
		$(5.76 \times 10^{-3})+$	$(1.33 \times 10^{-2})+$	$(1.27 \times 10^{-2})+$	$(7.12 \times 10^{-3})-$	$(6.32 \times 10^{-3})+$	(6.76×10^{-3})
+/−/=		2/8/2	2/9/1	2/8/2	0/9/3	2/6/4	

4.5. Quantify the Number of Mutation Strategies across Different Algorithms and Test Functions

As illustrated in Table 4, our algorithm retains a greater number of solutions compared to other algorithms across various test functions during the mutation-based offspring generation process. This demonstrates that our algorithm effectively mitigates resource waste. Furthermore, our algorithm secured first place in 6 out of the 12 test functions, further attesting to its effectiveness.

Table 4. Number of individuals eliminated/created during mutation.

	D	NSGA-II	MOEA/D	SPEA2	CDE-NSGA-II	CMWOA	NDE-NSGA-II
ZDT1	30	127/299	291/633	161/303	134/318	122/314	98/310
ZDT2	30	129/302	315/594	152/318	133/302	137/295	125/312
ZDT3	30	163/269	388/633	142/325	145/295	147/311	120/328
ZDT4	10	82/103	216/407	76/100	89/111	89/94	105/189
ZDT6	10	58/101	121/219	53/95	54/102	41/94	65/106
DTLZ1	7	8/70	36/237	8/69	10/75	20/73	8/77
DTLZ2	12	4/132	36/382	6/123	3/115	4/102	2/121
DTLZ3	12	44/126	43/347	33/117	28/113	28/108	16/126
DTLZ4	12	14/103	26/268	7/124	16/132	11/113	2/120
DTLZ5	12	7/122	13/343	9/113	11/126	13/120	6/134
DTLZ6	12	85/115	48/339	11/133	11/115	2/106	6/132
DTLZ7	12	102/193	298/587	103/222	90/230	80/233	123/241

5. Experiments and Analysis of Results

5.1. Study Area

The research area is situated in Hulan District, Harbin City, Heilongjiang Province, China (46.340683° N 126.795502° E), as shown in Figure 5. This region, located in northeastern China, falls within the continental monsoon climate of the northern temperate zone, exhibiting distinct cold, warm, dry, and wet seasons.

Figure 5. Location of the field of study.

Fine-tuning a variety of parameters is vital for accurately simulating the local growth environment. Maize (Longdan 96) has a plant height of 280 cm and an ear height of 100 cm. 18 leaves can be seen in adult plants. The number of rows per ear is 16–18, with teeth-shaped and yellow grains, and a weight of 34 g per hundred grains. It is suitable for planting in the first accumulated temperature zone of Heilongjiang Province (data sourced from Heilongjiang Academy of Agricultural Sciences). In this experiment, field data from 2015 were gathered, and the parameters in the variety parameter file were adjusted using a trial-and-error method. Weather data spanning from 2011 to 2015 for average optimization were employed. The weather data for 2015 are shown in Figure 6. The DSSAT model can effectively use these parameters to simulate the growth of local crops.

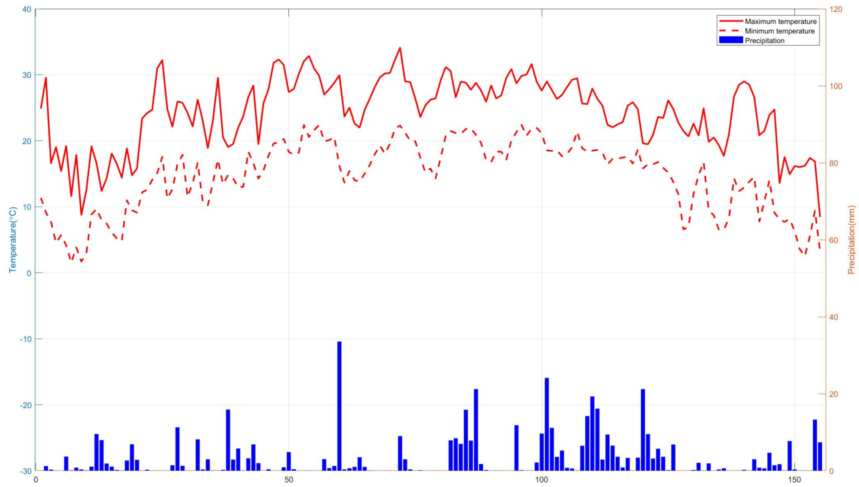

Figure 6. Precipitation and highest and lowest temperatures in 2015.

5.2. Objective Function

Multi-objective optimization problems involve maximizing or minimizing two or more objectives by adjusting one or more variables. In the context of crop production, decision-makers modify irrigation and fertilization methods to attain optimal outcomes. This study specifically addresses the timing and quantity of irrigation or fertilization in the field. The objective function is outlined as follows:

$$Max : Y = \frac{\sum_{i=0}^{N} DSSAT_i(i_{a_0}, \ldots, i_{a_j}, f_{a_0}, \ldots, f_{a_d}, D_i)}{N} \tag{11}$$

$$Min : I = \frac{\sum_{i=0}^{N} \sum_{n=0}^{j} (i_{a_n})}{N} \tag{12}$$

$$Min : F = \frac{\sum_{i=0}^{N} \sum_{m=0}^{d} (f_{a_m})}{N} \tag{13}$$

In the formula, Y is the yield, I is the total irrigation amount, F is the total nitrogen application amount, i_{a_n} is the one-time irrigation amount, f_{a_m} is the one-time nitrogen application amount, j is the irrigation amount, d is the nitrogen application amount, and N = 5 represents the number of years simulated. D_i is the time for irrigation and fertilization.

5.3. Optimization Strategies and Configuration

Symmetry also plays an important role in water and fertilizer irrigation in agriculture. Figure 7 shows the flowchart of optimizing water and fertilizer. We use the R language to drive the DSSAT model for optimization. Using the integrated method of water and fertilizer, the effect of different fertilizers on the maize yield was studied. The simulation situation is divided into two groups: rain irrigation and drip irrigation. We applied urea (N1), diammonium phosphate (N2), and ammonium nitrate (N3) separately. Maize undergoes five growth stages—seedling (VE), jointing (VJ), tasseling (VT), filling (R2), and physiological maturity (R6). Fertilization and irrigation are carried out during these stages. The dates for irrigation and fertilization are determined based on historical experience, but due to differences in weather between different years, we have set their historical experience dates to ±5 days. Considering the actual situation and based on historical experience, the sowing date of Longdan 96 is set on May 1st, and the harvest date is set on October 1st. The goal of each optimization strategy is to maximize production while minimizing resource waste. In the case of two objectives, the population is 100 with 100 iterations, and in the case of three objectives, the population is 300 with 100 iterations.

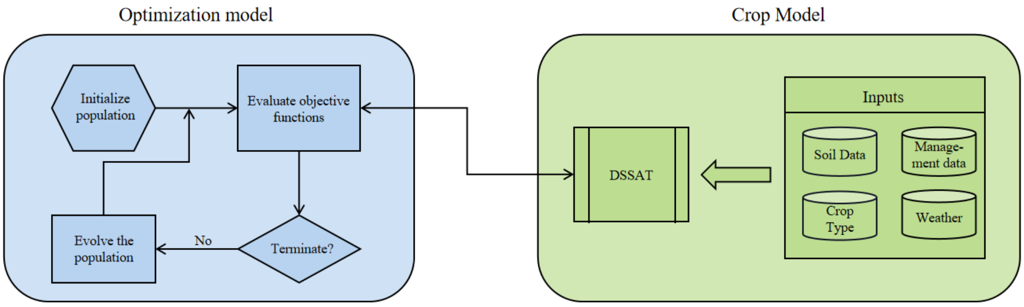

Figure 7. Flow chart of optimized water and fertilizer irrigation.

5.4. Result and Analysis

Figure 8 illustrates that in the absence of irrigation, the utilization of N1 fertilizer not only results in a higher yield (10,515 kg/ha) but also requires less fertilizer compared to the other two fertilizers. Furthermore, the enhanced algorithm identifies a more rational fertilization strategy. For instance, at the point of maximum yield (10,515 kg/ha), the original algorithm utilized 312 kg/ha of fertilizer, whereas the improved algorithm required only 264 kg/ha, reflecting a 15% reduction in fertilizer application compared to the original algorithm. This outcome substantiates the reliability and efficacy of the improved algorithm.

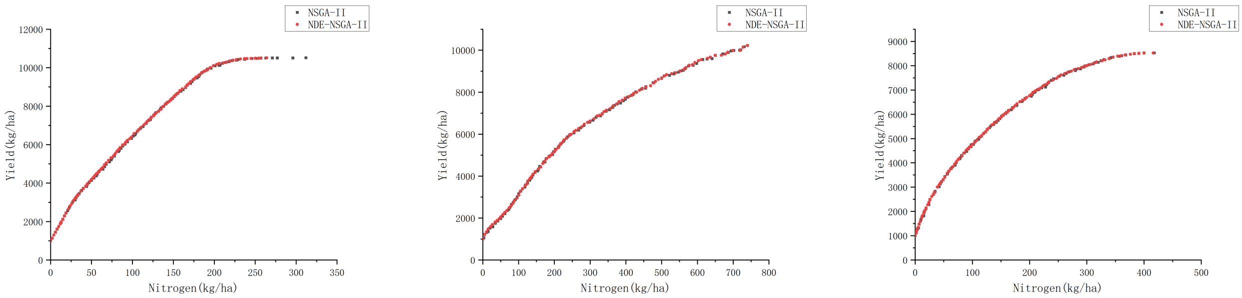

(**a**) N1 (**b**) N2 (**c**) N3

Figure 8. Comparison of fertilization strategies between NSGA-II algorithm and NDE-NSGA-II algorithm.

From Figure 9, it can be seen that under the comprehensive strategy of drip irrigation and fertilization, the highest yields of N1, N2, and N3 nitrogen fertilizers were 13,585 kg/ha, 13,589 kg/ha, and 13,587 kg/ha, respectively. This means that under irrigation conditions, all three fertilization methods can achieve higher yields. Compared with the original algorithm, the improved algorithm exhibits superior yield performance while minimizing resource waste to the greatest extent possible.

In addition, the improved algorithm provides decision-makers with more irrigation decision-making solutions and verifies its reliability. Given the relatively low resource consumption of N2 fertilizer, which has the lowest cost among the three types of fertilizers (see Table 5 for details), N2 fertilizer has become the preferred choice under irrigation strategies, improving its economic benefits. The optimal yield and resource consumption achieved by applying different fertilizers, coupled with historical experience, are detailed in Table 6, overall, applying N2 fertilizer and achieving the highest yield, with water consumption reduced by 37.5%, nitrogen application reduced by 8.3%, and yield increased by 5.9%.

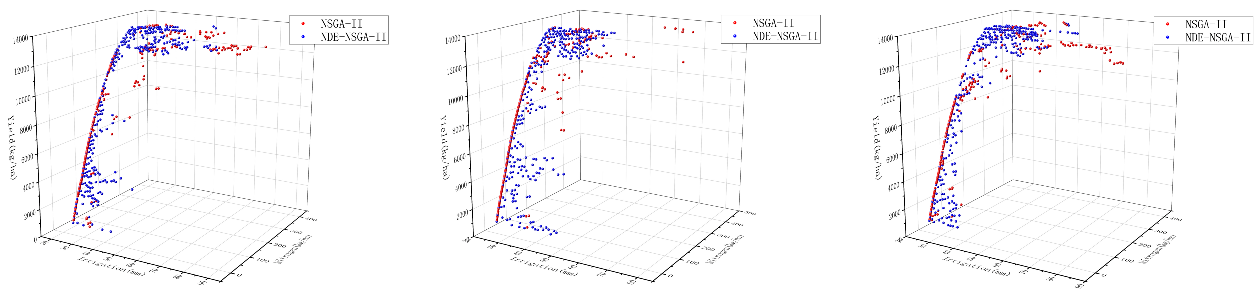

(**a**) N1 (**b**) N2 (**c**) N3

Figure 9. Comparison of irrigation and fertilization strategies between NSGA-II algorithm and NDE-NSGA-II algorithm.

Table 5. Different fertilizer prices.

N1 Costs (Yuan/kg)	N2 Costs (Yuan/kg)	N3 Costs (Yuan/kg)
3.98	2.65	3.82

Examining Table 6, it is evident that opting for the N2 fertilization strategy yields the highest output. However, in regions facing water scarcity, alternatives such as minimal irrigation or no irrigation strategies could be considered as viable options.

Table 6. Comparison of best-simulated irrigation and nitrogen fertilizer test results with best practices (using different fertilizers).

	Yield (kg/ha)		Yield Increase (%)	Total Irrigation (mm)		Irrigation Reduction (%)	Total Nitrogen (kg/ha)		Fertilization Reduction (%)
	Practices	Optimized Results		Practices	Optimized Results		Practices	Optimized Results	
N1	12,836	13,585	5.8%	80	55	31.3%	300	375	−25%
N2		13,589	5.9%		50	37.5%		275	8.3%
N3		13,587	5.5%		62	22.5%		277	7.7%

6. Discussion

The NDE-NSGA-II algorithm significantly outperforms traditional multi-objective optimization algorithms. It has demonstrated robust performance in test functions and excels in optimizing resource allocation strategies, such as crop irrigation and fertilization. However, the algorithm has certain limitations. Although NDE-NSGA-II improves convergence speed, its computational complexity is relatively high, particularly for large-scale optimization problems, which can lead to increased computational resource consumption. Additionally, the algorithm's performance may be sensitive to parameter settings, and improper parameter selection can affect optimization results, necessitating further research on parameter tuning and automation methods. Furthermore, this study primarily relies on simulation environments for testing, and the algorithm's performance in practical applications has not been fully validated, requiring further empirical research. In summary, the development of the NDE-NSGA-II algorithm is significant for multi-objective optimization, and its potential impact on agricultural applications underscores its practical value. However, further research is needed to address existing limitations and validate its effectiveness in real-world scenarios.

7. Conclusions

This article presents the NDE-NSGA-II algorithm as a solution for handling multi-objective problems. Specifically, chaotic mapping is utilized to enhance the initialization process. This is followed by the implementation of a point selection method based on norm and average distance elimination strategies, aiming to improve convergence and diversity within the population. The performance of the proposed NDE-NSGA-II is rigorously validated across 12 benchmark functions, each with distinct features. Comparative analyses are conducted against other state-of-the-art methods in the field of multi-objective problems (MOPs). The experimental results robustly affirm the effectiveness and reliability of the algorithm, showcasing its capability to simultaneously address multi-objective problems with high diversity and achieve commendable convergence. Finally, the NDE-NSGA-II algorithm, introduced in this paper, is applied to optimize maize-related scenarios, demonstrating superiority over the classical NSGA-II method. However, we only simulated an ideal corn water and fertilizer irrigation, which has certain limitations. In the future, we can consider using certain methods to predict weather changes and yield. These results further underscore the practical efficacy of the NDE-NSGA-II algorithm proposed in this study.

In the future, applying NDE-NSGA-II to more complex high-dimensional multi-objective problems will be a promising work. At the same time, further testing will be conducted on multi-objective problems in the real world, and the algorithm will be improved.

Author Contributions: Conceptualization, J.D. and R.L.; methodology, J.D.; software, D.C.; validation, X.W.; formal analysis, T.Z.; investigation, F.Y.; resources, J.D.; data curation, D.C.; writing—original draft preparation, R.L.; writing—review and editing, J.D.; visualization, R.L.; supervision, J.D.; project administration, X.W.; funding acquisition, D.C., R.L. and F.Y. All authors have read and agreed to the published version of the manuscript.

Funding: This research received no external funding.

Data Availability Statement: The data supporting this study's findings are available from the corresponding author upon request.

Conflicts of Interest: The authors declare no conflicts of interest.

References

1. Cai, Y.; Wang, J. Differential evolution with hybrid linkage crossover. *Inf. Sci.* **2015**, *320*, 244–287. [CrossRef]
2. Zhou, A.; Qu, B.Y.; Li, H.; Zhao, S.Z.; Suganthan, P.N.; Zhang, Q. Multiobjective evolutionary algorithms: A survey of the state of the art. *Swarm. Evol. Comput.* **2011**, *1*, 32–49. [CrossRef]
3. Pourvaziri, H.; Naderi, B. A hybrid multi-population genetic algorithm for the dynamic facility layout problem. *Appl. Soft. Comput.* **2014**, *24*, 457–469. [CrossRef]
4. Saborido, R.; Ruiz, A.B.; Luque, M. Global WASF-GA: An evolutionary algorithm in multiobjective optimization to approximate the whole pareto optimal front. *Evol. Comput.* **2017**, *25*, 309–349. [CrossRef] [PubMed]
5. Tran, K.D. An improved non-dominated sorting genetic algorithm-ii (ANSGA-II) with adaptable parameters. *Int. J. Intell. Syst. Technol. Appl.* **2009**, *7*, 347–369. [CrossRef]
6. Ahadzadeh, B.; Abdar, M.; Safara, F.; Khosravi, A.; Menhaj, M.B.; Suganthan, P.N. SFE: A simple, fast and efficient feature selection algorithm for high-dimensional data. *IEEE Trans. Evol. Comput.* **2023**, *27*, 1896–1911. [CrossRef]
7. Lin, Z.; Gao, K.; Wu, N.; Suganthan, P.N. Scheduling eight-phase urban traffic light problems via ensemble meta-heuristics and Q-learning based local search. *IEEE Trans. Intell. Transp. Syst.* **2023**, *24*, 14415–14426. [CrossRef]
8. Ma, Z.; Wu, G.; Suganthan, P.N.; Song, A.; Luo, Q. Performance assessment and exhaustive listing of 500+ nature-inspired metaheuristic algorithms. *Swarm Evol. Comput.* **2023**, *77*, 101248. [CrossRef]
9. Gad, A.G.; Houssein, E.H.; Zhou, M.C.; Suganthan, P.N.; Wazery, Y.M. Damping-assisted evolutionary swarm intelligence for industrial iot task scheduling in cloud computing. *IEEE Internet Things J.* **2023**, *11*, 1698–1710. [CrossRef]
10. Ma, H.; Zhang, Y.; Sun, S.; Liu, T.; Shan, Y. A comprehensive survey on NSGA-II for multi-objective optimization and applications. *Artif. Intell. Rev.* **2023**, *56*, 15217–15270. [CrossRef]
11. Li, W.; Zhang, T.; Wang, R.; Huang, S.; Liang, J. Multimodal multi-objective optimization: Comparative study of the state-of-the-art. *Swarm Evol. Comput.* **2023**, *77*, 101253. [CrossRef]
12. Deb, K.; Pratap, A.; Agarwal, S.; Meyarivan, T.A.M.T. A fast and elitist multiobjective genetic algorithm: NSGA-II. *IEEE Trans. Evol. Comput.* **2002**, *6*, 182–197. [CrossRef]
13. Zhang, Q.; Li, H. MOEA/D: A multiobjective evolutionary algorithm based on decomposition. *IEEE Trans. Evol. Comput.* **2007**, *11*, 712–731. [CrossRef]
14. Zitzler, E.; Laumanns, M.; Thiele, L. SPEA2: Improving the strength Pareto evolutionary algorithm. *TIK Rep.* **2001**, *103*, 10017663175.

15. Zhou, Y.; Fan, H. Research on multi objective optimization model of sustainable agriculture industrial structure based on genetic algorithm. *J. Intell. Fuzzy Syst.* **2018**, *35*, 2901–2907. [CrossRef]
16. Cheng, D.; Yao, Y.; Liu, R.; Li, X.; Guan, B.; Yu, F. Precision agriculture management based on a surrogate model assisted multiobjective algorithmic framework. *Sci. Rep.* **2023**, *13*, 1142. [CrossRef]
17. Song, J.; Li, J.; Yang, Q.H.; Mao, X.; Yang, J.; Wang, K. Multi-objective optimization and its application on irrigation scheduling based on AquaCrop and NSGA-II. *J. Hydraul. Eng.* **2018**, *49*, 1284–1295.
18. Llera, J.R.; Deb, K.; Runkle, E.; Xu, L.; Goodman, E. Evolving and comparing greenhouse control strategies using model-based multi-objective optimization. In Proceedings of the 2018 IEEE Symposium Series on Computational Intelligence (SSCI), Bangalore, India, 18–21 November 2018; pp. 1929–1936.
19. Liu, X.; Yang, D. Irrigation schedule analysis and optimization under the different combination of P and ET0 using a spatially distributed crop model. *Agric. Water Manag.* **2021**, *256*, 107084. [CrossRef]
20. White, J.W.; Alagarswamy, G.; Ottman, M.J.; Porter, C.H.; Singh, U.; Hoogenboom, G. An overview of CERES–sorghum as implemented in the crop system model version 4.5. *Agron. J.* **2015**, *107*, 1987–2002. [CrossRef]
21. Ritchie, J.T. Description and performance of CERES wheat: A user-oriented wheat yield model. *ARS Wheat Yield Proj.* **1985**, *8*, 159–175.
22. Otter-Nacke, S.; Ritchie, J.T.; Godwin, D.C.; Singh, U. *A User's Guide to CERES Barley—V2. 10*; International Fertilizer Development Center Simulation Manual: Muscle Shoals, AL, USA, 1991; IFDC-SM-3.
23. Liu, J.; Chen, X. An improved NSGA-II algorithm based on crowding distance elimination strategy. *Int. J. Comput. Intell. Syst.* **2019**, *12*, 513–518. [CrossRef]
24. Dos Santos Coelho, L.; Mariani, V.C. Use of chaotic sequences in a biologically inspired algorithm for engineering design optimization. *Expert Syst. Appl.* **2008**, *34*, 1905–1913. [CrossRef]
25. Yan, Z.; Jin, Q.; Zhang, Y.; Wang, Z.; Li, Z. An Improved Multi-Objective Harris Hawk Optimization with Blank Angle Region Enhanced Search. *Symmetry* **2022**, *14*, 967. [CrossRef]
26. Kaveh, A.; Ilchi Ghazaan, M.; Saadatmand, F. Colliding bodies optimization with Morlet wavelet mutation and quadratic interpolation for global optimization problems. *Eng. Comput.* **2022**, *38*, 2743–2767. [CrossRef]
27. Zitzler, E.; Deb, K.; Thiele, L. Comparison of multiobjective evolutionary algorithms: Empirical results. *Evol. Comput.* **2000**, *8*, 173–195. [CrossRef] [PubMed]
28. Deb, K.; Thiele, L.; Laumanns, M.; Zitzler, E. Scalable multi-objective optimization test problems. In Proceedings of the 2002 Congress on Evolutionary Computation, CEC'02 (Cat. No. 02TH8600), Honolulu, HI, USA, 12–17 May 2002; Volume 1, pp. 825–830.
29. Zeng, N.; Song, D.; Li, H.; You, Y.; Liu, Y.; Alsaadi, F.E. A competitive mechanism integrated multi-objective whale optimization algorithm with differential evolution. *Neurocomputing* **2021**, *432*, 170–182. [CrossRef]
30. Li, M.; Yao, X. Quality evaluation of solution sets in multiobjective optimisation: A survey. *ACM Comput. Surv. (CSUR)* **2019**, *52*, 26. [CrossRef]
31. Ishibuchi, H.; Masuda, H.; Tanigaki, Y.; Nojima, Y. Modified distance calculation in generational distance and inverted generational distance. In Proceedings of the Evolutionary Multi-Criterion Optimization: 8th International Conference, EMO 2015, Guimarães, Portugal, 29 March–1 April 2015; Proceedings, Part II 8; Springer International Publishing: New York, NY, USA, 2015; pp. 110–125.
32. Tian, Y.; Cheng, R.; Zhang, X.;Li, M.; Jin, Y. Diversity assessment of multi-objective evolutionary algorithms: Performance metric and benchmark problems [research frontier]. *IEEE Comput. Intell. Mag.* **2019**, *14*, 61–74. [CrossRef]
33. Zitzler, E.; Thiele, L. Multiobjective optimization using evolutionary algorithms—A comparative case study. In Proceedings of the International Conference on Parallel Problem Solving from Nature, Berlin, Heidelberg, 27–30 September 1998; Springer: Berlin/Heidelberg, Germany, 1998; pp. 292–301.

Disclaimer/Publisher's Note: The statements, opinions and data contained in all publications are solely those of the individual author(s) and contributor(s) and not of MDPI and/or the editor(s). MDPI and/or the editor(s) disclaim responsibility for any injury to people or property resulting from any ideas, methods, instructions or products referred to in the content.